Discrete Supply Modulation of a Three-Stage K-Band PA

Maxwell R. Duffy[1], Gregor Lasser[2], and Zoya Popović[3]

Department of Electrical, Computer, and Energy Engineering, University of Colorado, Boulder, USA

[1] Maxwell.Duffy@colorado.edu [2] Gregor.Lasser@colorado.edu [3] Zoya@colorado.edu

***Abstract* — A three-stage K-band GaN MMIC amplifier with over 20 dB of saturated gain, greater than 4 W peak output power, and a peak PAE over 40 % is characterized using supply modulation. A discrete supply modulator is used to track the 50 MHz noise-like signal used for testing. Drain supply modulation increases the efficiency by 9 percentage points and, through the use of a flat-gain shaping function, does not degrade the linearity compared to the static supply case for the same output power. An adaptive shaping function for the discrete supply modulator further improves supply modulation performance in back-off. This work demonstrates an improvement in efficiency without the need for pre-distortion and, to the best of the authors' knowledge, is the first demonstration of supply modulation on a GaN PA at K-Band.**

***Keywords* — Power amplifiers, efficiency, GaN, K-band, linearity, noise power ratio, discrete supply modulation.**

I. Introduction

Transmitters for satellite communication systems are required to be both highly efficient and capable of very linear operation. Efficiency is especially critical in phased array due to the large number of active elements and thermal limitations. While continuous supply modulators have been used to improve transmitter efficiency, their bandwidth limitations are well known, e.g. [1], [2], and do not lend themselves well to the broadband signals used in satellite communications. Discrete supply modulators have shown promise for improving efficiency for broadband signals but the discrete voltage levels introduce non-linearities that need to be corrected [3], [4].

A three-stage GaN K-band PA [5] is tested at 19.8 GHz with drain supply modulation as shown in Fig. 1. An efficient GaN MMIC discrete supply modulator [6] is used to generate the drain supply voltage, allowing efficient transmission of a 50 MHz noise-like signal. The tracking function is designed to maximize amplifier linearity while simultaneously improving efficiency to eliminate the need for pre-distortion. To the best of the authors' knowledge, this is the first demonstration of supply modulation on a GaN PA at K-Band.

II. Amplifier and Discrete Supply Modulator

A K-Band amplifier designed in the Qorvo 150 nm GaN process is used for obtaining the experimental results in this paper. The process utilizes a 100 μm SiC substrate with internal source vias in the transistors. The amplifier has three stages with a 1:2:8 staging ratio, over 20 dB of saturated gain, over 4 W peak output power, and peak efficiencies ranging from 40-45 % from 18.5 to 24 GHz. The amplifier is designed for a supply voltage of V_{D}=20 V with a 100 mA/mm quiescent current. A photo of the MMIC is shown in Fig.2a and a more detailed explanation of the amplifier design and characterization can be found in [5].

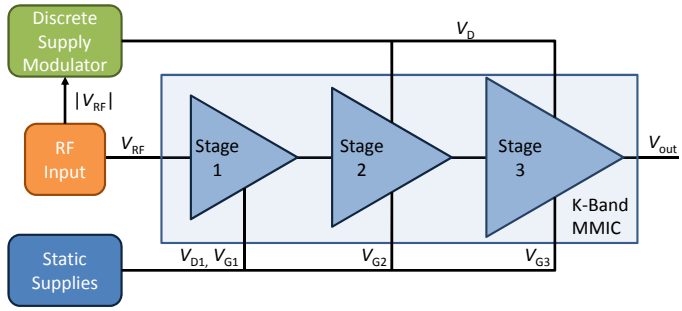

Fig. 1. Block diagram of a a three-stage PA supply-modulated transmitter with a dynamic drain voltage VD on the second and third stage, while first stage supply is static ($V_{\mathrm{D1}} = \mathrm{const}$. The three gates are statically biased by V_{G1}, V_{G2}, and V_{G3}.

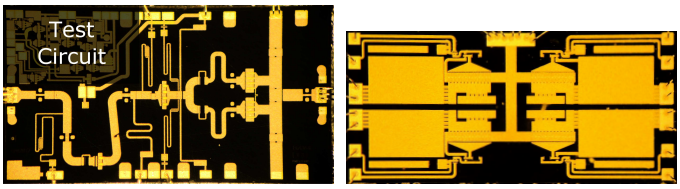

(a) (b)

Fig. 2. Fabricated GaN MMICs: (a) K-Band amplifier (4 mm×2 mm) and 4-level discrete supply modulator (5.4 mm×2.6 mm).

The discrete supply modulator (DSM) is also designed in a Qorvo 150 nm GaN on 100 μm SiC process, in an earlier version of the process with circular vias. The modulator power stage consists of 4 hard-switching transistors connected to 4 individual supply voltages. Each transistor is toggled on individually to apply a voltage to the output node of the supply modulator. An on chip snubber network is used on the DC supply side of the switching transistors to reduce ringing during transitions. Two of the transistors in the switching cell make use of a modified active pull-up driver while two make use of an active pull-up driver to minimize driver losses in the circuit. For composite efficiency measurements two efficiency metrics will be shown, one with and one without driver losses. A photo of the supply modulator MMIC is given in Fig.2b and a more detailed explanation of the circuit design and characterization can be found in [6].

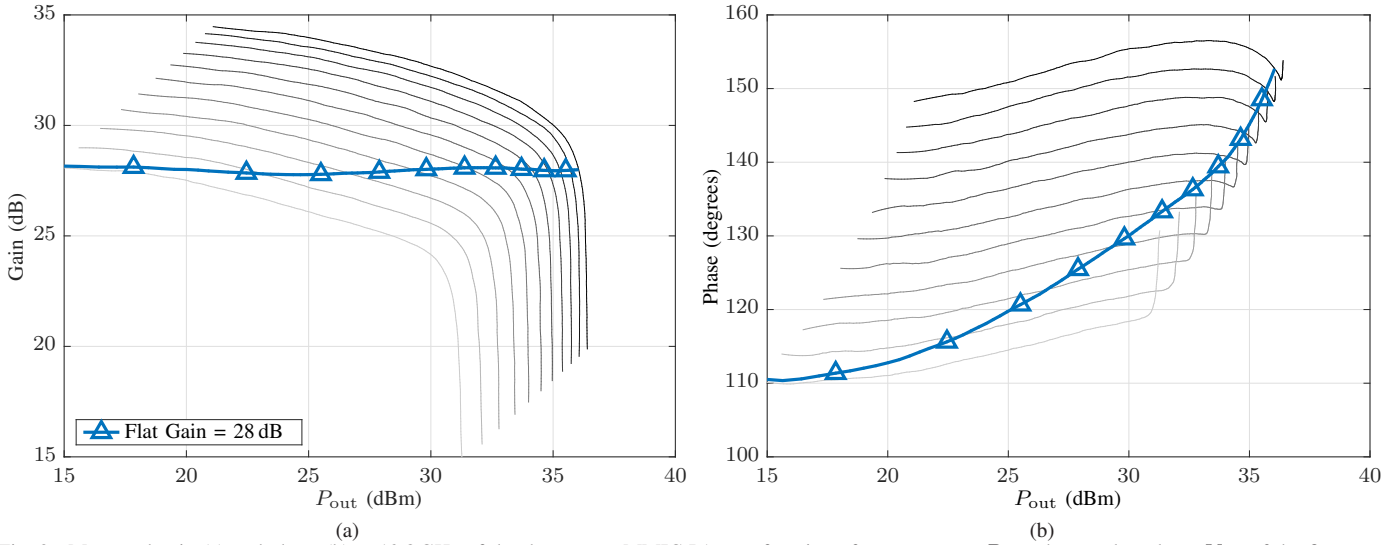

Fig. 3. Measured gain (a) and phase (b) at 19.8 GHz of the three-stage MMIC PA as a function of output power P_{out}. the supply voltage V_{D1} of the first stage is kept constant at 20 V, while $V_{\text{D2}} = V_{\text{D3}}$ are simultaneously varied from 10-20 V. The static performance is shown in grey lines in 1-V steps darkening with higher V_{D}. While the gain amplitude stays flat at 28 dB, the phase is expected to vary by 40°.

III. Shaping Function Design

The amplifier is characterized for several supply voltages (6-28 V) using a VNA with an external test-set. Measurement results give absolutely calibrated static AM/AM and AM/PM data for a sweep of input powers. The drain supply voltages of most interest are 10-20 V shown in Fig. 3. Here the drain voltage is modulated to maintain a flat gain over drive power (Fig. 3). The gain value is set by the lowest modulation voltage, here 10 V is used for a gain of 28 dB. The voltage is allowed to vary by 10 V up to $V_{\text{Dmax}} = 20$ V, minimizing the negative effects on linearity from the signal discretization.

Static characterization is used to create the shaping functions (SF) shown in Fig. 4. The continuous flat gain SF is discretized for use with the 4-level DSM. For back-off input power levels, the peak power $\hat{P}_{\text{in}}$ does not reach the level where V_{D}=20 V occurs. In these cases the DSM is being underutilized as fewer of the voltage levels are being used and the discrete voltages levels are not adapted well for the real voltage swing. To mitigate this a modified shaping function is designed when the amplifier is backed-off from saturation. This new adaptive shaping function (ASF) should further improve amplifier performance in back-off. The PDFs of a noise like signal are superimposed on top of the SFs for an amplifier being driven to compression and average power $\overline{P}_{\text{in}}$=-6 dBm.

IV. Measurement Method and Results

The supply modulated PA is characterized using the setup shown in Fig. 5. An external source generates a 2.5 GHz clock signal used by the bit pattern generator (BPG). From this input the BPG creates clock signals for the arbitrary waveform generator (AWG) allowing 800 ps resolution between the two instruments. The BPG creates control signals for the 4-level DSM while the AWG generates baseband IQ data which is then upconverted by a vector signal generator (VSG). Signal data is received by a vector signal analyzer (VSA) which also provides

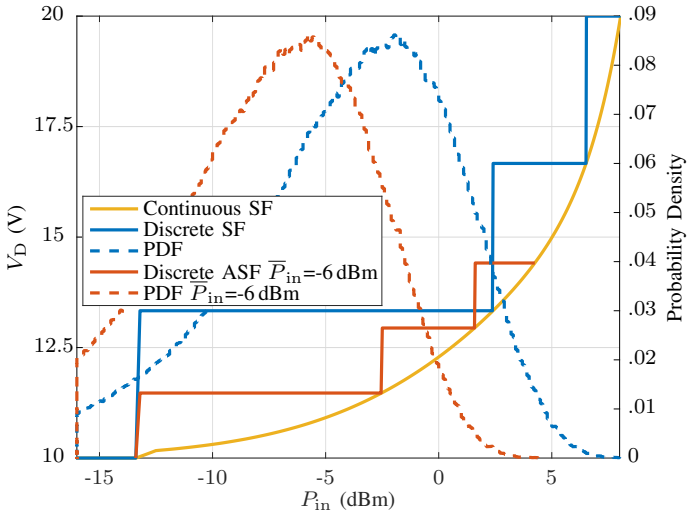

Fig. 4. Shaping functions derived from static amplifier measurements. Solid lines show three shaping functions: continuous; discretized; and discretized for $\overline{P}_{\text{in}}$=-6 dBm. This third shaping function is designed for improved efficiency at lower input power levels, compared to a V_{D} that varies from 10-20 V. PDFs for both discrete cases are shown in dashed lines.

the 10 MHz reference clock for the setup. Power measurements are calibrated up to the plane of reference of the DUT on both the input and output.

The 4-level DSM is used to provide the dynamic drain supply voltage. The DSM is connected to the K-band amplifier through spring loaded pins. The interconnect is made as short as possible to minimize added bias line inductance. The DSM provides the V_{D} only for the second and third stage while the first stage uses a static 20 V supply voltage. The RF and drain supply paths are aligned using the methods described in [7]. The switching speed of the DSM is limited to 150 MHz by the ISO721M digital isolator chip which is used to level shift the output of the BPG to the switching voltage needed by

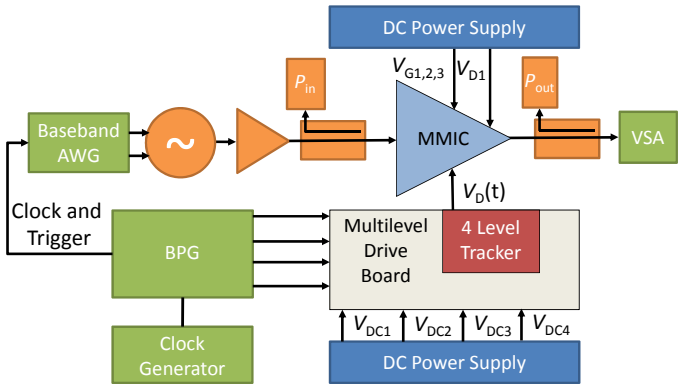

Fig. 5. Block diagram of test setup. Gate bias voltages 1, 2, and 3 are independently set. Drain supply voltage V_{D1} is static, while dynamic drain voltages $V_{D2} = V_{D3}$ are provided by a 4-level tracker controlled by a bit pattern generator (BPG) that commutates four external voltages, $V_{DC1}, V_{DC2}, V_{DC3}$, and V_{DC4}.

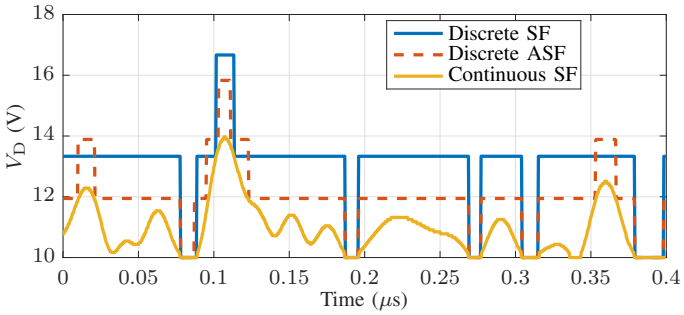

Fig. 6. Time domain V_D for a 50 MHz noise-like signal at $\overline{P}_{in}$=-6 dBm. Three shaping functions are shown: one for discretized 10-20 V variation; the second in which the voltage variation is changed to better reflect the signal statistics; and the third is a continuous function.

the 4-level tracker. The time domain V_D for different shaping functions can be seen in Fig. 6.

A 50 MHz noise-like signal with a PAPR of greater than 10 dB is generated using the method described in [8]. Testing is done at 19.8 GHz and noise power ratio (NPR) is used as the metric of linearity. The amplifier output is captured in both the spectral and time domain for each data point. The receive bandwidth of the setup is limited by the VSAs maximum 170 MHz sampling frequency for IQ data. Received time domain data is time and phase aligned before being processed. Additionally a full spectral measurement (DC-44 GHz) is done at every power level to check for stability.

Fig. 7 shows power sweep results for three cases: a static 20 V supply, supply modulation (SM), and supply modulation using an adaptive shaping function (ASF SM). Static measurements successfully predicted the dynamic gain of the amplifier (28 dB) using SM. For P_{out} >24 dBm the SM cases have virtually identical NPR to the static supply case with NPR actually improving over the static supply case from 24-30 dBm. The ASF case improves NPR, PAE, and flattens gain for P_{out} <26 dBm, which is where V_D does not reach the 20 V level using SM. Without driver losses taken into account PAE improves by 9pp for supply modulation, or 4.5pp when

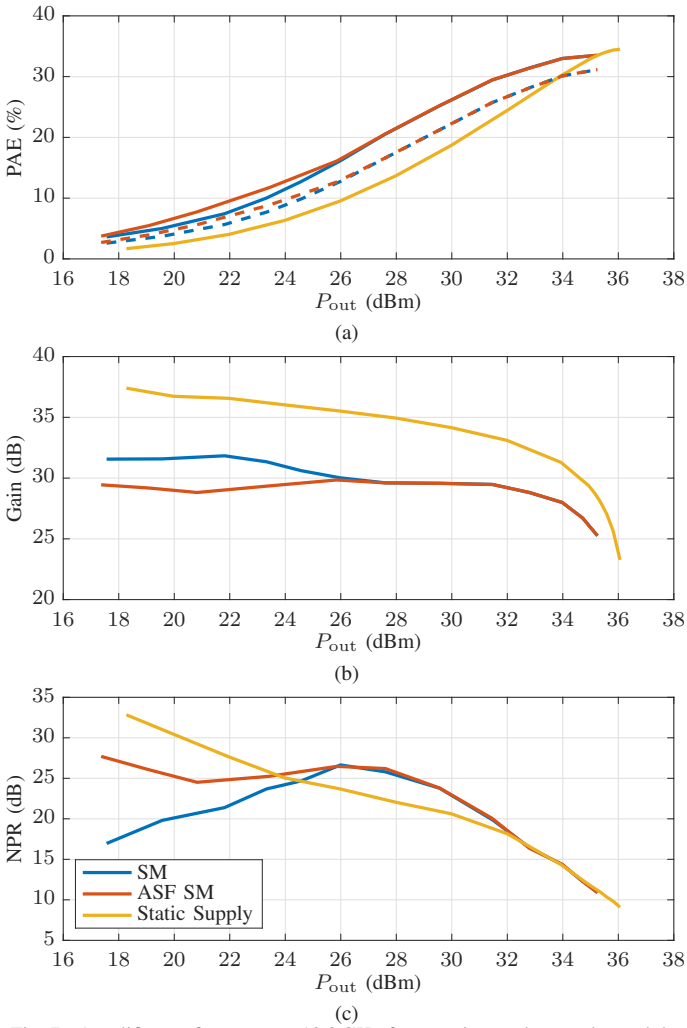

Fig. 7. Amplifier performance at 19.8 GHz for a static supply, supply modulation (SM), and SM using an adaptive shaping function (ASF). Performance is shown over P_{out} for (a) PAE (efficiency measurements without driver losses are solid while those including driver losses are dashed), (b) gain, and (c) NPR.

factoring in driver losses. A more efficient DSM architecture with reduced driver losses would further benefit transmmitter efficiency.

AM/AM and AM/PM data for two power levels and the three cases of supply modulation can be seen in Fig.8, with the following interesting conclusions:

- In the case of lower output power, at P_{out}=22 dBm, both discrete supply modulation shaping functions give improvement in AM/AM distortion, as seen in Fig.8a-8b.
- Further, the adaptive shaping function (ASF) SM case offers benefits over the SM case for AM/AM, flattening out the gain response. The AM/PM distortion is also reduced for the ASF SM case, while Fig.7a shows simultaneous improvement in efficiency.
- At higher drive levels SM and ASF SM result in the same shaping function so only one case is shown.
- In the case of higher output power, P_{out}=28 dBm, the AM/AM and AM/PM for the static static supply and

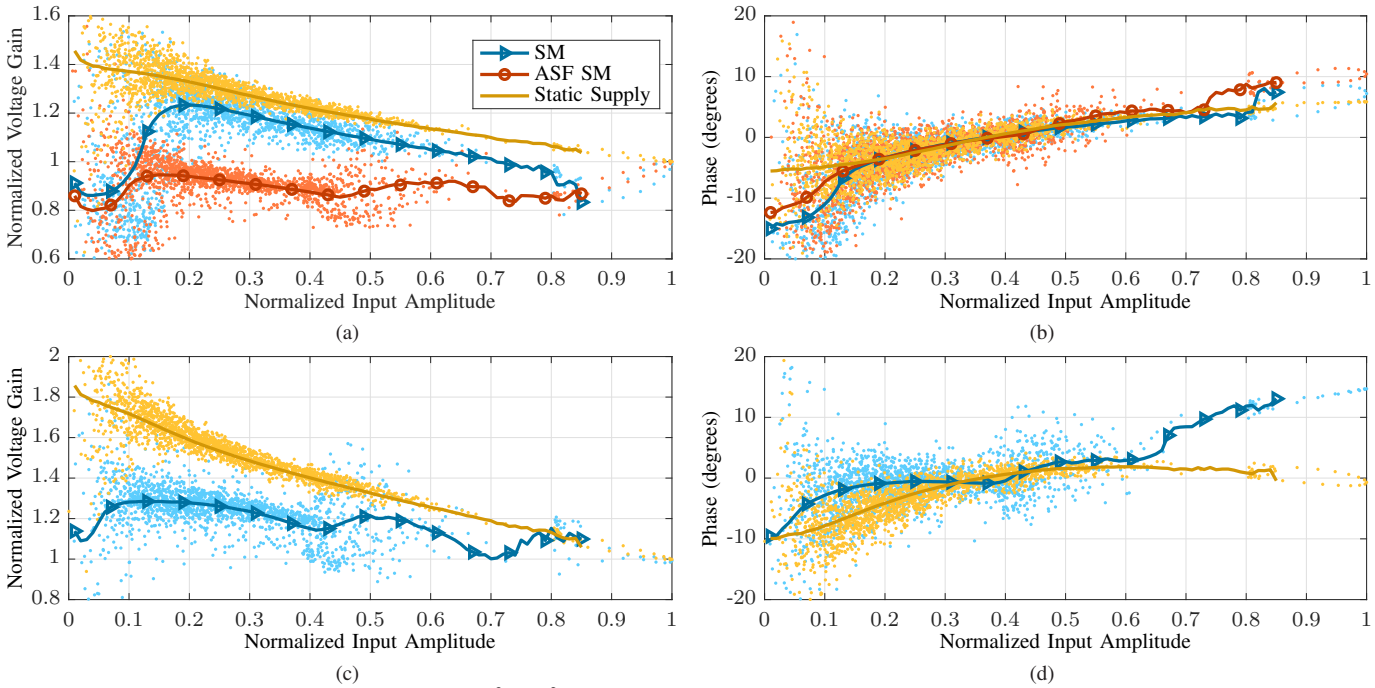

Fig. 8. Measured performance at 19.8 GHz for Pout={22,28} dBm showing (a,c) AM/AM and (b,d) AM/PM, respectively, for a 50-MHz NPR signal with a PAPR>10 dB. The blue data points show performance with supply modulation, red points shows supply modulation with an adaptive shaping function, and yellow shows a static supply. The discrete points are faded and a darker trend line is superimposed for clarity. The horizontal axis is normalized to maximum V_{in}. Voltage gain is normalized to unity for the peak input amplitude. At Pout=28 dBm, the two supply modulation cases give identical performance so only one is plotted.

discretized supply modulation are shown in Fig. 8c-8d, with clear improvement in gain amplitude linearity when the PA is supply modulated.

- SM reduces gain variation when compared with the static supply case, but this does *not* come at the expense of efficiency, which is increased as shown in Fig.7a.
- This reduction in gain variation is complemented by a rise in phase variation as predicted by static measurements. At this power level, the NPR for the supply-modulated case exceeds the NPR for the static supply case.

V. Conclusion

A three-stage K-band GaN MMIC amplifier is characterized at 19.8 GHz using a DSM for a 50 MHz signal and improvement in efficiency is shown. For P_{out} >24 dBm the linearity of the static and SM cases are virtually identical while SM increases the efficiency by 9pp. It is shown that in back-off the shaping function between the drain supply and input power can be improved by adapting the SF to account for the actual voltage swing at the amplifier input. This is especially relevant in a DSM where the selected discrete voltage levels determine the resolution of the tracking function.

References

[1] J. Jeong *et al.*, "Wideband envelope tracking power amplifiers with reduced bandwidth power supply waveforms and adaptive digital predistortion techniques," *IEEE Trans. Microw. Theory Techn.*, vol. 57, no. 12, pp. 3307–3314, 2009.

[2] Y. Zhang, M. Rodríguez, and D. Maksimović, "100 MHz, 20 V, 90% efficient synchronous buck converter with integrated gate driver," in *Energy Conversion Congress and Exposition (ECCE), 2014 IEEE*. IEEE, 2014, pp. 3664–3671.

[3] N. Wolff, O. Bengtsson, M. Schmidt, M. Berroth, and W. Heinrich, "Linearity analysis of a 40 W class-G-modulated microwave power amplifier," in *Microwave Integrated Circuits Conference (EuMIC), 2015 10th European*. IEEE, 2015, pp. 365–368.

[4] C. Florian, T. Cappello, R. P. Paganelli, D. Niessen, and F. Filicori, "Envelope tracking of an RF high power amplifier with an 8-level digitally controlled GaN-on-Si supply modulator," *IEEE Trans. Microw. Theory Techn.*, vol. 63, no. 8, pp. 2589–2602, 2015.

[5] M. R. Duffy, G. Lasser, M. Roberg, and Z. Popović, "A 4-W K-band 40% PAE three-stage MMIC power amplifier," in *2018 IEEE BiCMOS and Compound Semiconductor Integrated Circuits and Technology Symposium (BCICTS)*. IEEE, 2018, pp. 144–147.

[6] A. Sepahvand, P. Momenroodaki, Y. Zhang, Z. Popović, and D. Maksimović, "Monolithic multilevel GaN converter for envelope tracking in RF power amplifiers," in *Energy Conversion Congress and Exposition (ECCE), 2016 IEEE*. IEEE, 2016, pp. 1–7.

[7] G. Lasser, M. Duffy, and Z. Popović, "Dynamic dual-gate bias modulation for linearization of a high-efficiency multi-stage PA," *IEEE Trans. Microw. Theory Techn.*, accepted for publication.

[8] T. Reveyrand *et al.*, "A novel experimental noise power ratio characterization method for multicarrier microwave power amplifiers," in *ARFTG Conference Digest-Spring, 55th*, vol. 37. IEEE, 2000, pp. 1–5.